

Non-centrosymmetric Rubidium Rare-earth Nitrates $\text{Rb}_2\text{RE}(\text{NO}_3)_5 \cdot 4\text{H}_2\text{O}$: Crystal Growth and Optical Properties

Ladislav Bohatý,^{*[a]} Peter Held,^[a] and Petra Becker^[a]

Dedicated to Professor Gerd Meyer on the Occasion of His 60th Birthday

Keywords: Rubidium rare earth nitrate; Crystal growth; Non-centrosymmetric crystal; Refractive indices; SHG phase matching

Abstract. Large single crystals of optical quality of the isomorphic, non-centrosymmetric, monoclinic (space group *Cc*) compounds $\text{Rb}_2\text{La}(\text{NO}_3)_5 \cdot 4\text{H}_2\text{O}$ and $\text{Rb}_2\text{Ce}(\text{NO}_3)_5 \cdot 4\text{H}_2\text{O}$ were grown. The determination of precise refractive indices and their dispersion in the wavelength region 0.365–1.083 μm allowed a detailed analysis of phase matching conditions for nonlinear optical second har-

monic generation. Type I phase matching conditions can be realized in both crystals for a wide frequency range. Our X-ray structure determination of $\text{Rb}_2\text{Nd}(\text{NO}_3)_5 \cdot 4\text{H}_2\text{O}$ and $\text{Rb}_2\text{Pr}(\text{NO}_3)_5 \cdot 4\text{H}_2\text{O}$ shows that both compounds are isomorphic to the lanthanum and cerium compounds.

Introduction

Among the alkali rare earth nitrates, members of the family of the polar orthorhombic compounds of type $\text{K}_2\text{RE}(\text{NO}_3)_5 \cdot 2\text{H}_2\text{O}$ (with $\text{RE} = \text{La} - \text{Nd}$) turned out to be attractive crystals for efficient nonlinear optical frequency conversion through second harmonic generation (SHG) [1, 2]. Whereas isomorphic compounds with rubidium are unknown, tetrahydrates $\text{Rb}_2\text{RE}(\text{NO}_3)_5 \cdot 4\text{H}_2\text{O}$ that crystallize with monoclinic symmetry *Cc* were described for $\text{RE} = \text{La}$ and Ce by [3, 4]. Already in 1907, these compounds had been reported first by *Wyrouboff* [5], who gave a detailed morphological description and pointed out their isomorphism to the corresponding ammonium compounds $(\text{NH}_4)_2\text{RE}(\text{NO}_3)_5 \cdot 4\text{H}_2\text{O}$ ($\text{RE} = \text{La} - \text{Nd}$) [6–10]. The compounds were reported with (centrosymmetric) monoclinic-prismatic symmetry that was maintained for the ammonium compounds in later X-ray structure determinations [11–13]. *Wyrouboff* [5] also reported on a probably isomorphic rubidium “didymium” compound, the isomorphism of $\text{Rb}_2\text{Pr}(\text{NO}_3)_5 \cdot 4\text{H}_2\text{O}$ and $\text{Rb}_2\text{Nd}(\text{NO}_3)_5 \cdot 4\text{H}_2\text{O}$ with the lanthanum and cerium compounds was stated also by [14], however, no structure determination of the praseodymium and neodymium compounds is given in literature.

At this point the question arises, whether the rubidium rare earth nitrates tetrahydrates are isomorphous with the corresponding ammonium compounds (and are therefore centrosymmetric) or the above cited description [3, 4] in the polar space group *Cc* is correct. Using small crystals of $\text{Rb}_2\text{RE}(\text{NO}_3)_5 \cdot 4\text{H}_2\text{O}$ ($\text{RE} = \text{La}, \text{Ce}$), which were synthesized in a first step of our investigation, we could detect unambiguously piezoelectricity of the crystals as well as the generation of second harmonic of laser light, thus giving a strong proof of the non-centrosymmetry of the rubidium compounds. These first results encouraged the growth of large single crystals of the colorless compounds $\text{Rb}_2\text{La}(\text{NO}_3)_5 \cdot 4\text{H}_2\text{O}$ and $\text{Rb}_2\text{Ce}(\text{NO}_3)_5 \cdot 4\text{H}_2\text{O}$ for linear and nonlinear optical investigations. In addition, we studied the crystal structure of the corresponding praseodymium and neodymium compound.

Results and Discussion

Crystal Structure

Our crystal structure analysis reveals that $\text{Rb}_2\text{Nd}(\text{NO}_3)_5 \cdot 4\text{H}_2\text{O}$ and $\text{Rb}_2\text{Pr}(\text{NO}_3)_5 \cdot 4\text{H}_2\text{O}$ are isomorphic to the corresponding lanthanum and cerium compounds [3, 4], with space group symmetry *Cc* and lattice parameters as summarized in Table 1. The prominent structural unit is a distorted icosahedral coordination polyhedron of the rare earth [REO_{12}], where ten oxygen ligands belong to five bidentately coordinating nitrate groups and the remaining two oxygen ligands are oxygen atoms of water molecules, leading to a structural building block $[\text{RE}(\text{NO}_3)_5(\text{H}_2\text{O})_2]^{2-}$, see Figure 1. The arrangement of the $[\text{NO}_3]$ groups around the central rare earth cation gives an approximately

* Prof. Dr. L. Bohatý
Fax: +49-221-470-4963
E-Mail: ladislav.bohaty@uni-koeln.de
[a] Institut für Kristallographie
Universität zu Köln
Zùlpicher Str. 49 b
50674 Köln, Germany

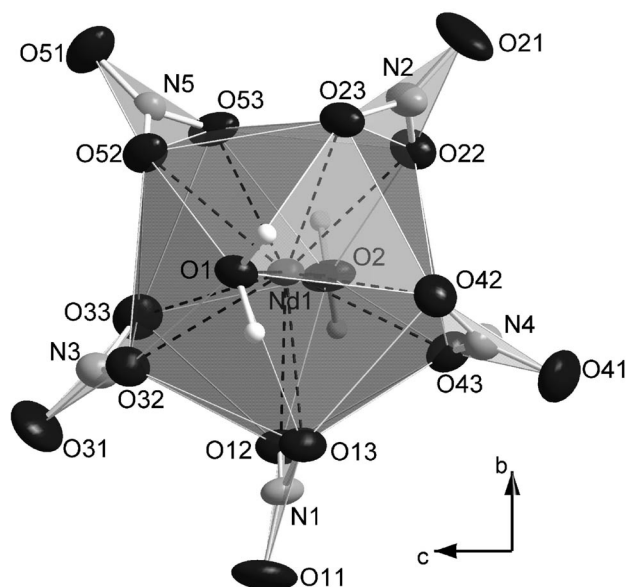
Table 1. Crystal structure data of monoclinic $\text{Rb}_2\text{RE}(\text{NO}_3)_5 \cdot 4\text{H}_2\text{O}$ with $\text{RE} = \text{La} - \text{Nd}$.

	La ^{a)}	Ce ^{b)}	Pr ^{c)}	Nd ^{c)}
$a/\text{Å}$	11.092(4)	11.050(1)	11.0223(8)	11.0011(6)
$b/\text{Å}$	8.984(2)	8.977(1)	8.9691(5)	8.9601(3)
$c/\text{Å}$	17.863(6)	17.859(2)	17.861(2)	17.840(3)
$\beta/^\circ$	100.85(1)	100.877(9)	100.929(9)	100.966(7)
$V/\text{Å}^3$	1748.2	1739.6(2)	1733.7(3)	1726.3(3)
Z	4	4	4	4
$\rho/\text{g} \cdot \text{cm}^{-3}$	2.49	2.648	2.659	2.683

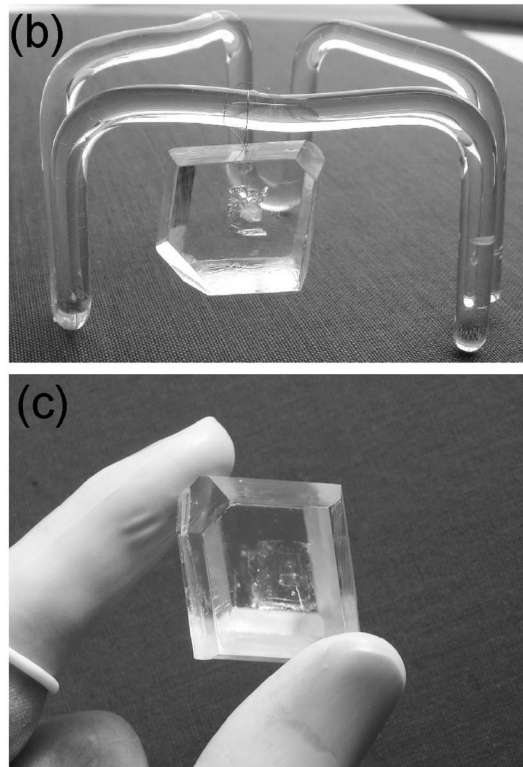
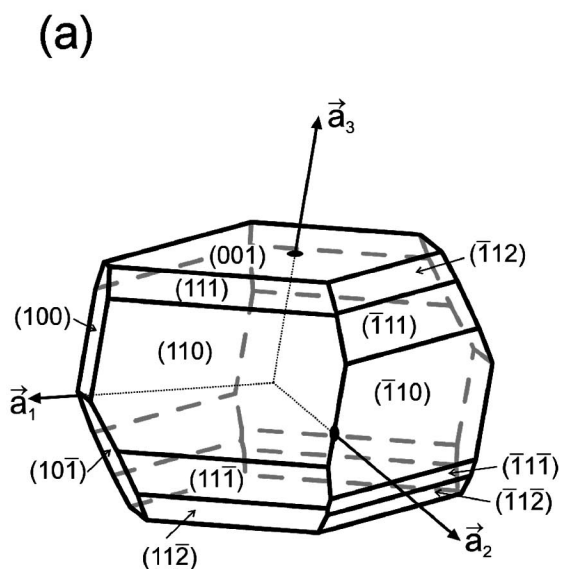
a) Vigdorichik et al., 1992 [3]; b) Audebrand et al., 1996 [4]; c) this paper.

radial paddle wheel-like geometry, which was also described for $\text{Cs}_2\text{La}(\text{NO}_3)_5 \cdot 2\text{H}_2\text{O}$ [15] and for the ammonium compounds $(\text{NH}_4)_2\text{RE}(\text{NO}_3)_5 \cdot 4\text{H}_2\text{O}$ ($\text{RE} = \text{La}, \text{Ce}, \text{Nd}$) [11–13] and $(\text{NH}_4)\text{La}(\text{NO}_3)_5 \cdot 3\text{H}_2\text{O}$ [11]. The $[\text{RE}(\text{NO}_3)_5(\text{H}_2\text{O})_2]$ groups are arranged in layers parallel (001) that alternate with layers of rubidium cations and H_2O along the c -axis. The resulting sheet-like structure corresponds to a distinct cleavage of the crystals parallel to (001).

In the nonlinear optically attractive potassium compounds of type $\text{K}_2\text{RE}(\text{NO}_3)_5 \cdot 2\text{H}_2\text{O}$ (with $\text{RE} = \text{La} - \text{Nd}$) a similar structural building block $[\text{RE}(\text{NO}_3)_5(\text{H}_2\text{O})_2]$ is present. Here, however, the arrangement of the $[\text{NO}_3]$ groups differs markedly from that in the rubidium com-

**Figure 1.** Coordination polyhedron $[\text{Nd}(\text{NO}_3)_5(\text{H}_2\text{O})_2]$ in $\text{Rb}_2\text{Nd}(\text{NO}_3)_5 \cdot 4\text{H}_2\text{O}$. Non hydrogen atoms are shown as 50 % probability displacement ellipsoids and hydrogen atoms as spheres with arbitrary radius for clarity.

pounds $\text{Rb}_2\text{RE}(\text{NO}_3)_5 \cdot 4\text{H}_2\text{O}$ (with $\text{RE} = \text{La} - \text{Nd}$), and no radial paddle wheel-like geometry but a pronounced polar arrangement is found [16].

**Figure 2.** (a) Typical morphology of grown crystals of $\text{Rb}_2\text{La}(\text{NO}_3)_5 \cdot 4\text{H}_2\text{O}$ and $\text{Rb}_2\text{Ce}(\text{NO}_3)_5 \cdot 4\text{H}_2\text{O}$; face indices and the crystallographic reference system $\{\vec{a}_i\}$ are indicated. (b) Example of a grown crystal of $\text{Rb}_2\text{La}(\text{NO}_3)_5 \cdot 4\text{H}_2\text{O}$, fixed with platinum wire to the seed crystal holder. (c) Example of a grown crystal of $\text{Rb}_2\text{Ce}(\text{NO}_3)_5 \cdot 4\text{H}_2\text{O}$. The region of the seed crystal is clearly visible in both crystals. Crystals shown in (b) and (c) are approximately of the same size.

Crystal Growth

From our growth experiments large single crystals of dimensions up to $4 \times 4 \times 3$ cm and a mass of 50–75 g for both compounds, $\text{Rb}_2\text{La}(\text{NO}_3)_5 \cdot 4\text{H}_2\text{O}$ and $\text{Rb}_2\text{Ce}(\text{NO}_3)_5 \cdot 4\text{H}_2\text{O}$, were obtained, see Figure 2b and Figure 2c. In the progress of the growth process, the disturbances in the region around the initial seed crystal, which are visible in Figure 2b and Figure 2c, vanished, and crystals of high optical quality, which allow the measurement of high-precision refractive indices, resulted. The morphology of the crystals is dominated by the pedions (001) and (00 $\bar{1}$) and domes {110} and $\{1\bar{1}0\}$. Additionally, the pedions (100), ($\bar{1}00$), (10 $\bar{1}$), ($\bar{1}01$) and domes {111}, {1 $\bar{1}\bar{1}$ }, {11 $\bar{2}$ }, { $\bar{1}\bar{1}2$ }, { $\bar{1}\bar{1}1$ }, { $\bar{1}\bar{1}\bar{1}$ } and { $\bar{1}\bar{1}\bar{2}$ } occur, see Figure 2a. The well-developed faces of the crystals were used as reference for the preparation of oriented samples. Crystal physical properties reported in this work are related to a Cartesian system $\{\vec{e}_i\}$ that is defined with respect to the crystallographic system $\{\vec{a}_i\}$ as follows: $\vec{e}_2 \parallel \vec{a}_2$, $\vec{e}_3 \parallel \vec{a}_3$, $\vec{e}_1 = \vec{e}_2 \times \vec{e}_3$. In our crystals positive directions of \vec{e}_1 and \vec{e}_3 correspond with a positive sign of the piezoelectric constant d_{111} and d_{333} , respectively.

Optical Properties

Refractive index data were measured at 11 discrete wavelengths and were corrected with the refractive index of air (see Experimental Section). All data given here correspond to the corrected values. A modified Sellmeier equation of the type

$$n^2(\lambda) = D_1 + \frac{D_2}{(\lambda^2 - D_3)} - D_4\lambda^2$$

was used to fit the refractive indices. In Figure 3, the principal refractive indices and their dispersion, together with the Sellmeier functions are illustrated, the Sellmeier coefficients are given in Table 2. The transparency range of the crystals extends from approx. 0.315 μm for $\text{Rb}_2\text{La}(\text{NO}_3)_5 \cdot 4\text{H}_2\text{O}$ and approx. 0.355 μm for $\text{Rb}_2\text{Ce}(\text{NO}_3)_5 \cdot 4\text{H}_2\text{O}$ in the UV (50 % transmission) to about 1.40 μm in the infrared range, where first absorption bands occur for both compounds (see insets of Figure 3).

Table 2. Sellmeier coefficients for crystals of $\text{Rb}_2\text{La}(\text{NO}_3)_5 \cdot 4\text{H}_2\text{O}$ and $\text{Rb}_2\text{Ce}(\text{NO}_3)_5 \cdot 4\text{H}_2\text{O}$; the wavelength in the Sellmeier equation is in μm (χ^2 is the sum of the squares of the residuals of the fit).

	D_1	D_2	D_3	D_4	χ^2
$\text{Rb}_2\text{La}(\text{NO}_3)_5 \cdot 4\text{H}_2\text{O}$					
n_1^0	2.27643(8)	0.01633(2)	0.0308(1)	0.00906(7)	6.1×10^{-11}
n_2^0	2.2732(2)	0.01668(6)	0.0304(3)	0.0083(2)	3.1×10^{-10}
n_3^0	2.20288(6)	0.01458(2)	0.0300(1)	0.00663(5)	3.4×10^{-11}
$\text{Rb}_2\text{Ce}(\text{NO}_3)_5 \cdot 4\text{H}_2\text{O}$					
n_1^0	2.2868(4)	0.0165(1)	0.0341(5)	0.0095(3)	1.3×10^{-9}
n_2^0	2.2878(6)	0.0172(2)	0.0348(10)	0.0086(4)	1.4×10^{-9}
n_3^0	2.2145(3)	0.01493(8)	0.0322(4)	0.0071(2)	8.0×10^{-10}

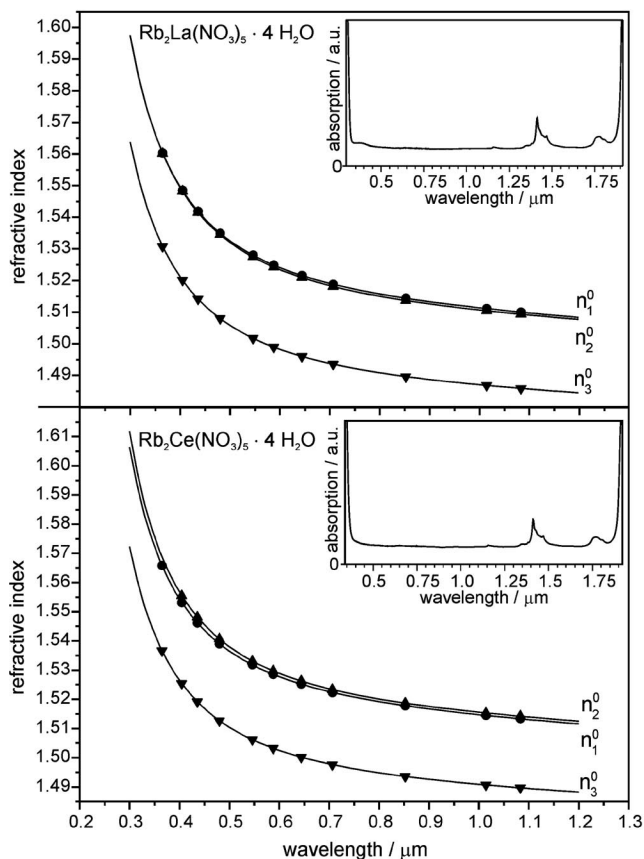


Figure 3. Principal refractive indices and their dispersion, together with unpolarized absorption spectra (insets) of crystals of $\text{Rb}_2\text{La}(\text{NO}_3)_5 \cdot 4\text{H}_2\text{O}$ (upper panel) and of $\text{Rb}_2\text{Ce}(\text{NO}_3)_5 \cdot 4\text{H}_2\text{O}$ (lower panel). Symbols indicate experimental refractive index data, lines indicate the fitted Sellmeier functions.

Crystals of $\text{Rb}_2\text{La}(\text{NO}_3)_5 \cdot 4\text{H}_2\text{O}$ and $\text{Rb}_2\text{Ce}(\text{NO}_3)_5 \cdot 4\text{H}_2\text{O}$ are biaxial negative with a small birefringence $\Delta n = |n_1^0 - n_2^0|$. In monoclinic crystals the orientation of the directions where the principal refractive indices of the crystals are found, i.e. the orientation of the principal axes of the optical indicatrix denoted by $\{\vec{e}_i^0\}$ in this work, is only fixed for \vec{e}_2^0 whereas the orientation of \vec{e}_1^0 and \vec{e}_3^0 varies within the plane (010) with wavelength of light. This wavelength-dependent dispersion of the orientation is given here as the angle Φ between the axis \vec{e}_3 ($\parallel \vec{a}_3$) and the principal axis \vec{e}_3^0 of the optical indicatrix (i.e. the extinction angle of the crystal with respect to the \vec{a}_3 -axis for a light wave propagation along \vec{e}_2). In Figure 4, the mutual orientation of the crystallographic reference system $\{\vec{a}_i\}$, the crystal physical Cartesian system $\{\vec{e}_i\}$ and the system of principal axes of the optical indicatrix $\{\vec{e}_i^0\}$ is sketched for the title crystals of this work. The wavelength-dependent rotation of the principal axes \vec{e}_1^0 and \vec{e}_3^0 around the \vec{e}_2 axis is illustrated by the wavelength dispersion of the angle Φ in Figure 5. Observed with white light this effect is visible on (010) plates of the crystals as bluish or reddish colors when

the crystals are slightly rotated off the position of maximum extinction in both directions between crossed polarizers. The angle between the optic axes (named $2V_\alpha$ in the following, see Figure 4) of $\text{Rb}_2\text{La}(\text{NO}_3)_5 \cdot 4\text{H}_2\text{O}$ increases with wavelength in the visible and slightly decreases again in the IR region (see Figure 6), the plane of the optic axes is $(\vec{e}_1^0, \vec{e}_3^0)$, i.e. (010). For $\text{Rb}_2\text{Ce}(\text{NO}_3)_5 \cdot 4\text{H}_2\text{O}$, $2V_\alpha$ decreases in the visible and slightly increases again in the IR (see Figure 6), here, the plane of the optic axes is $(\vec{e}_2^0, \vec{e}_3^0)$, i.e. the plane is rotated by 90° compared to that in $\text{Rb}_2\text{La}(\text{NO}_3)_5 \cdot 4\text{H}_2\text{O}$, as it is visualized in Figure 4. As a consequence of this result, the possibility to design a monoclinic crystal with optically uniaxial behavior within a certain wavelength range by the synthesis of mixed crystals $\text{Rb}_2(\text{La,Ce})(\text{NO}_3)_5 \cdot 4\text{H}_2\text{O}$ of appropriate ratio of La:Ce appears.

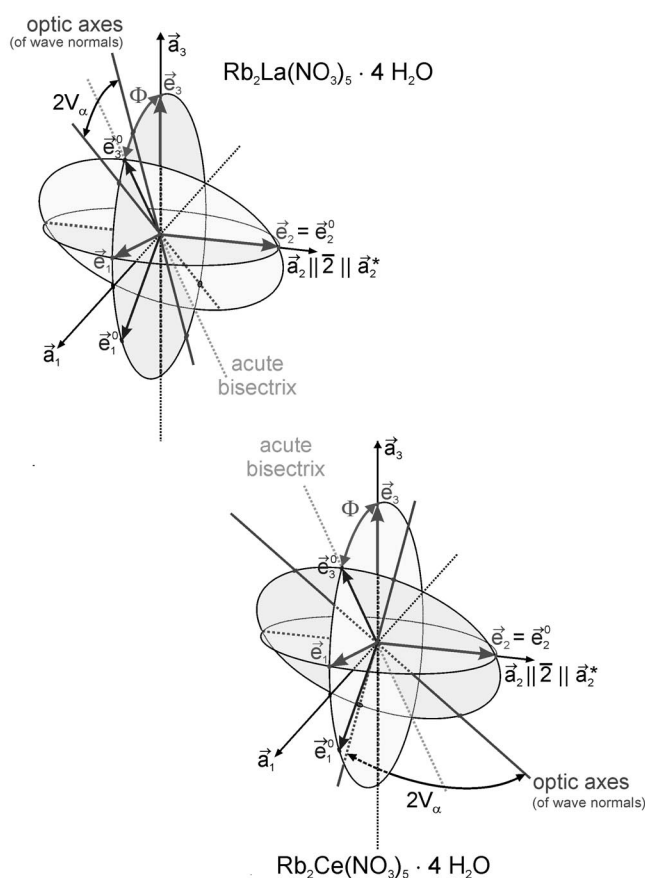


Figure 4. Mutual orientation of the crystallographic reference system $\{\vec{a}_i\}$, the crystal physical Cartesian system $\{\vec{e}_i\}$ and the system of principal axes of the optical indicatrix $\{\vec{e}_i^0\}$ for crystals of $\text{Rb}_2\text{La}(\text{NO}_3)_5 \cdot 4\text{H}_2\text{O}$ and $\text{Rb}_2\text{Ce}(\text{NO}_3)_5 \cdot 4\text{H}_2\text{O}$.

The high-precision refractive indices (with error less than 1×10^{-4}) and their dispersion allow an analysis of conditions for phase matching of different nonlinear optical frequency conversion processes. Herein, we focus in particular on the conditions for collinear second harmonic generation (SHG). Based on the birefringence $|n_1^0 - n_3^0|$ and $|n_2^0 - n_3^0|$, respectively, collinearly phase matched SHG pro-

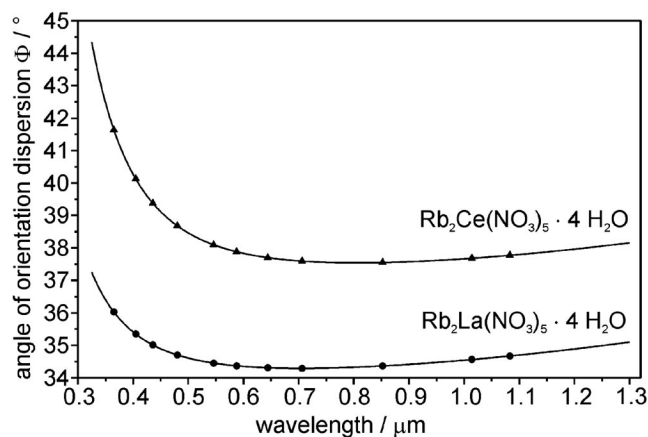


Figure 5. Wavelength dispersion of the orientation angle Φ ($= \chi_{\vec{e}_3, \vec{a}_3}$) for crystals of $\text{Rb}_2\text{La}(\text{NO}_3)_5 \cdot 4\text{H}_2\text{O}$ and $\text{Rb}_2\text{Ce}(\text{NO}_3)_5 \cdot 4\text{H}_2\text{O}$. Symbols: calculated from experimental data; lines: calculated from Sellmeier coefficients.

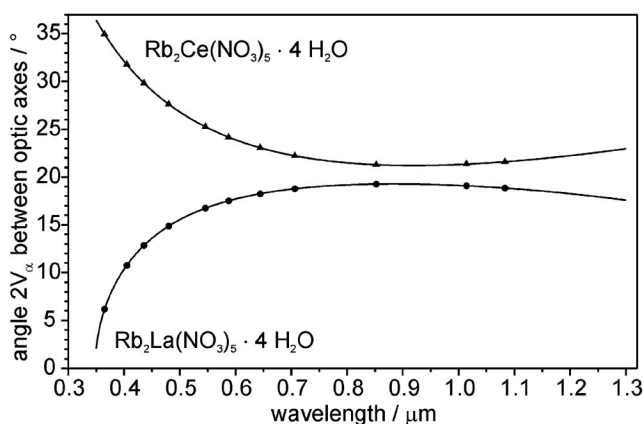


Figure 6. Wavelength dispersion of the acute angle $2V_\alpha$ between the optic axes of $\text{Rb}_2\text{La}(\text{NO}_3)_5 \cdot 4\text{H}_2\text{O}$ and $\text{Rb}_2\text{Ce}(\text{NO}_3)_5 \cdot 4\text{H}_2\text{O}$. Symbols: calculated from experimental data; lines: calculated from Sellmeier coefficients.

cesses of both types, type I phase matching (with ss-f interaction; s = slow wave, f = fast wave) and type II phase matching (with sf-f interaction) can be realized in both crystals, $\text{Rb}_2\text{La}(\text{NO}_3)_5 \cdot 4\text{H}_2\text{O}$ and $\text{Rb}_2\text{Ce}(\text{NO}_3)_5 \cdot 4\text{H}_2\text{O}$. However, type II phase matching is limited to the IR region where absorption already occurs in both crystals. Phase matching loci for several wavelengths of the fundamental wave are presented as Hobden plots (i.e. stereographic projection using the reference system $\{\vec{e}_i^0\}$ [17]) for both crystals in Figure 7. Non-critical phase matching type I is possible for a wavelength of $0.876 \mu\text{m}$ of the fundamental wave with wave normal \vec{k} parallel to \vec{e}_2^0 and at $0.889 \mu\text{m}$ for \vec{k} parallel to \vec{e}_1^0 in $\text{Rb}_2\text{La}(\text{NO}_3)_5 \cdot 4\text{H}_2\text{O}$. In $\text{Rb}_2\text{Ce}(\text{NO}_3)_5 \cdot 4\text{H}_2\text{O}$, non-critical phase matching type I can be realized at $0.887 \mu\text{m}$ for \vec{k} parallel to \vec{e}_1^0 and at $0.902 \mu\text{m}$ for \vec{k} parallel to \vec{e}_2^0 . The point group symmetry m of the crystals allows non-zero effective coefficients $d_{\text{eff}}^{\text{SHG}}$ of the SHG tensor for both directions of non-critical

phase matching type I in the crystals, e.g. d_{311}^{SHG} for incidence along \vec{e}_2^0 and d_{322}^{SHG} for incidence along \vec{e}_1^0 . The difference in wavelength for non-critical phase matching between $\text{Rb}_2\text{La}(\text{NO}_3)_5 \cdot 4\text{H}_2\text{O}$ and $\text{Rb}_2\text{Ce}(\text{NO}_3)_5 \cdot 4\text{H}_2\text{O}$ of 26 nm for incidence along \vec{e}_2^0 shows that by synthesis of mixed crystals $\text{Rb}_2(\text{La,Ce})(\text{NO}_3)_5 \cdot 4\text{H}_2\text{O}$ the wavelength for non-critical phase matching can be fine-tuned to a desired value within this range.

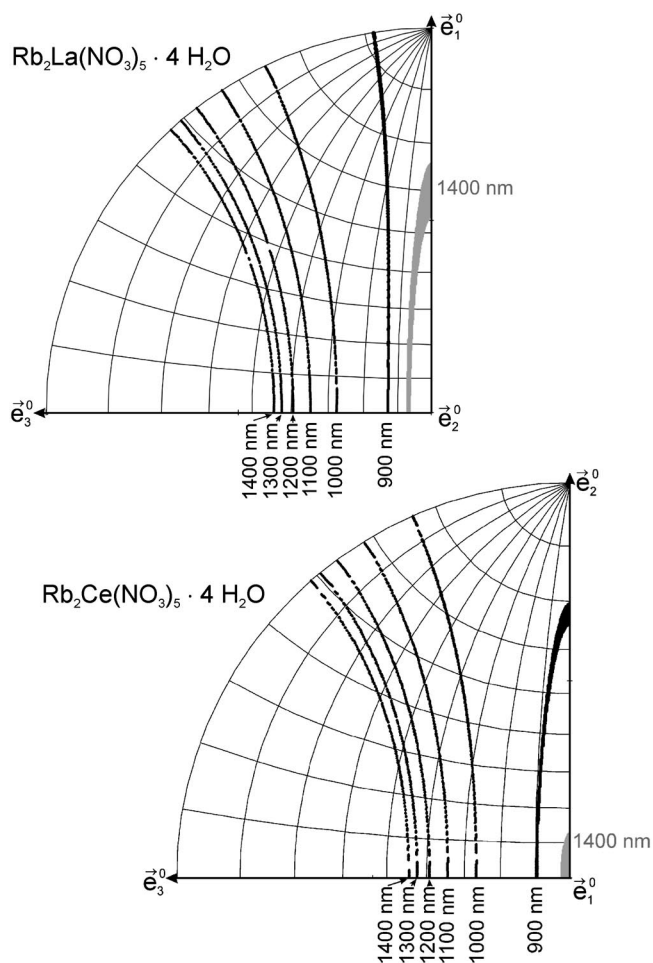


Figure 7. Stereographic projections of phase matching loci for collinear second harmonic generation (Hobden plots) for different fundamental wavelengths in $\text{Rb}_2\text{La}(\text{NO}_3)_5 \cdot 4\text{H}_2\text{O}$ (upper panel) and $\text{Rb}_2\text{Ce}(\text{NO}_3)_5 \cdot 4\text{H}_2\text{O}$ (lower panel). Loci of type I phase matching are marked in black, for type II phase matching in grey color.

Conclusions

The results of this work prove that the rubidium rare earth nitrates tetrahydrates $\text{Rb}_2\text{RE}(\text{NO}_3)_5 \cdot 4\text{H}_2\text{O}$ form an isomorphic series of non-centrosymmetric crystals for $\text{RE} = \text{La} - \text{Nd}$. Since the lanthanum and the cerium compounds (that are non-absorbing in the visible spectral range) can be grown to large single crystals of high quality and allow the realization of phase matched second harmonic generation, we can qualify these crystals as promis-

ing new nonlinear optical materials. In a forthcoming work the nonlinear optical susceptibility tensor [d_{ijk}^{SHG}] will be determined on the example of the lanthanum compound. An extension of the isomorphic series to a samarium compound seems highly improbable, to the best of our knowledge no crystal structure is known with samarium in dodecimal oxygen coordination [SmO_{12}]. Indeed, for the system $\text{RbNO}_3/\text{Sm}(\text{NO}_3)_3/\text{H}_2\text{O}$ only a dihydrate of composition $\text{Rb}_2\text{Sm}(\text{NO}_3)_5 \cdot 2\text{H}_2\text{O}$ (probably triclinic) is reported in literature [18], its crystal structure, however, is not given.

Experimental Section

Crystal Growth

Large single crystals of $\text{Rb}_2\text{La}(\text{NO}_3)_5 \cdot 4\text{H}_2\text{O}$ and $\text{Rb}_2\text{Ce}(\text{NO}_3)_5 \cdot 4\text{H}_2\text{O}$ were grown from saturated aqueous solutions with a stoichiometric ratio of the constituents (2 $\text{RbNO}_3 + 1 \text{La}(\text{NO}_3)_3$ or $1\text{Ce}(\text{NO}_3)_3$) and a small addition (ca. 5 %) of HNO_3 . Lanthanum nitrate was synthesized by dissolving La_2O_3 (Chempur, 99.99 %) in nitric acid, the cerium nitrate was purchased as hexahydrate, $\text{Ce}(\text{NO}_3)_3 \cdot 6\text{H}_2\text{O}$ (Chempur, 99.9 %) and commercially available rubidium nitrate (CERAC Inc., 99.9 %) was used. The growth process was performed for both compounds in 3 L crystallization vessels, held at constant temperature of 41 °C, by slow controlled evaporation of the solvent. The evaporation rate was adjusted to achieve a linear growth rate of approximately $0.3 \text{ mm} \cdot \text{day}^{-1}$. Seed crystals were suspended on platinum wire. In our experiments a growth period of 10–16 weeks was typically applied.

Small crystals of $\text{Rb}_2\text{Nd}(\text{NO}_3)_5 \cdot 4\text{H}_2\text{O}$ and $\text{Rb}_2\text{Pr}(\text{NO}_3)_5 \cdot 4\text{H}_2\text{O}$ suitable for X-ray structure determination were synthesized at 20 °C from aqueous solutions of the nitrates RbNO_3 and $\text{RE}(\text{NO}_3)_3$ ($\text{RE} = \text{Nd, Pr}$) in stoichiometric ratio 2 Rb : 1 RE with ca. 5 % HNO_3 added. The solutions of the rare earth nitrates were prepared by dissolving of Nd_2O_3 (Alfa, 99.9 %) and Pr_6O_{11} (Alfa Aesar, 99.9 %), respectively, in nitric acid using a small surplus of HNO_3 . All four compounds $\text{Rb}_2\text{RE}(\text{NO}_3)_5 \cdot 4\text{H}_2\text{O}$ are sensitive to humidity, especially the praseodymium and neodymium compounds.

Optical Properties

Crystals of monoclinic symmetry, such as $\text{Rb}_2\text{La}(\text{NO}_3)_5 \cdot 4\text{H}_2\text{O}$ and $\text{Rb}_2\text{Ce}(\text{NO}_3)_5 \cdot 4\text{H}_2\text{O}$, possess three principal refractive indices n_1^0, n_2^0, n_3^0 . They were determined by the prism method and normal incidence using two prisms with incidence face (010) (prism I) and (001) (prism II), respectively, for each compound. Measurements with the prisms I yield n_1^0 and n_3^0 , measurements with prisms II yield n_2^0 and n' with a value between n_1^0 and n_3^0 . For both compounds, data were collected at 11 discrete wavelengths in the region between $0.365 \mu\text{m}$ and $1.083 \mu\text{m}$ with a goniometer-spectrometer system (Möller-Wedel). The measured data were corrected for the refractive index of air and its dispersion by $n^{\text{corr}} = n^{\text{meas}} \cdot n^{\text{air}}$, using data from [19]. The extinction angle with respect to the edge between the faces (010) and (001), which has the direction of \vec{a}_1 , was measured on a plate (010) with a polarizing microscope. Unpolarized absorption spectra were collected with single crystal plates (010) of both compounds using a Varian Carey 05E equipment.

Crystal Structure Determination

$\text{Rb}_2\text{Pr}(\text{NO}_3)_5 \cdot 4\text{H}_2\text{O}$: Unit cell parameters of a cube-shaped single crystal ($0.35 \times 0.26 \times 0.24$ mm) were obtained by least-squares refinement from accurate angular settings of 25 reflection ($20.78^\circ < \theta < 23.76^\circ$) located and centred on a four-circle diffractometer. Room temperature intensity data of 10174 reflections were collected with a Enraf–Nonius MACH3 diffractometer [20] with $\omega/2\theta$ scan technique and graphite monochromatized Mo- K_α radiation ($\lambda = 0.7107 \text{ \AA}$) within the full hemisphere ($-15 \leq h \leq 15$, $-12 \leq k \leq 12$, $-25 \leq l \leq 25$; $2\theta < 30.41^\circ$). Preliminary investigations confirm a lattice centering, therefore only reflections with $h + k = 2n$ were measured. The data were averaged to give 5239 unique reflections ($R_{\text{int}} = 0.056$). Three standard reflections monitored periodically every 100 reflections showed no significant variation in position and intensity (max 3.72 %). Lorentz, polarisation and empirical absorption correction via psi-scan of nine reflections were applied ($\mu = 8.495 \text{ mm}^{-1}$, $T_{\text{min}} = 0.8204$, $T_{\text{max}} = 0.9995$, $F(000) = 1312$). The monoclinic space group Cc (No. 9) was proven to be consistent with the systematic absences in the original intensity data. Refinement was performed using full-matrix least-squares on F^2 with anisotropic displacement factors for non-hydrogen atoms, a structure factor weighting scheme and secondary isotropic extinction. Most of the non-hydrogen atoms were located using direct methods, remaining atoms were found in Fourier maps. In difference Fourier synthesis the strongest peaks corresponded (according to the stereochemical data) to possible positions of hydrogen and were identified as hydrogen atoms. All hydrogen atoms were restrained in length ($0.95(2) \text{ \AA}$) and constrained in the isotropic displacement parameter (1.2 times U_{equiv} of the bonded oxygen atom). The anisotropic refinement of 269 parameters (4055 reflections with $I_0 > 4\sigma(I_0)$) yielded a residual $R(F) = 0.0349$, $R_w(F^2) = 0.0691$ and $S = 1.048$ ($(\Delta/\sigma)_{\text{max}} = (\Delta/\sigma)_{\text{min}} = 0.000$). The Flack parameter is equal to $-0.00(1)$. The final difference map showed no unusual features ($\Delta\rho_{\text{max}} = 1.085 \text{ e} \cdot \text{\AA}^{-3}$, $\Delta\rho_{\text{min}} = -0.660 \text{ e} \cdot \text{\AA}^{-3}$). All calculation were performed on a DEC 300 AXP and a 786 PC computer using the WingX [21] and SHELX97 [22] program systems.

$\text{Rb}_2\text{Nd}(\text{NO}_3)_5 \cdot 4\text{H}_2\text{O}$: Procedures of the measurement of the crystal parameter, the data collection and refinement of the structure are similar to those used in the structure determination of $\text{Rb}_2\text{Pr}(\text{NO}_3)_5 \cdot 4\text{H}_2\text{O}$. A suitable single crystal ($0.36 \times 0.28 \times 0.27$ mm) was carefully selected under a polarizing microscope and mounted in a glass capillary. The cell parameters were obtained by 25 reflection ($20.74^\circ < \theta < 24.95^\circ$). 10139 measured reflections (within a 2θ range of 30.40°) were averaged to give 5222 unique reflections ($R_{\text{int}} = 0.049$, decay 2.37 %) corrected by absorption correction ($\mu = 8.717 \text{ mm}^{-1}$, $T_{\text{min}} = 0.7331$, $T_{\text{max}} = 0.9990$, $F(000) = 1316$). The anisotropic refinement of 269 parameters (4416 reflections with $I_0 > 4\sigma(I_0)$) yielded a residual $R(F) = 0.0270$, $R_w(F^2) = 0.0562$ and $S = 1.038$ ($(\Delta/\sigma)_{\text{max}} = (\Delta/\sigma)_{\text{min}} = 0.000$). The Flack parameter is equal to $-0.013(9)$. The final differ-

ence remains unremarkable ($\Delta\rho_{\text{max}} = 1.053 \text{ e} \cdot \text{\AA}^{-3}$, $\Delta\rho_{\text{min}} = -1.027 \text{ e} \cdot \text{\AA}^{-3}$).

Further details of the crystal structure investigations are available from the Fachinformationszentrum Karlsruhe, 76344 Eggenstein-Leopoldshafen, Germany on quoting the depository numbers CSD-420181 ($\text{Rb}_2\text{Nd}(\text{NO}_3)_5 \cdot 4\text{H}_2\text{O}$) and CSD-420187 ($\text{Rb}_2\text{Pr}(\text{NO}_3)_5 \cdot 4\text{H}_2\text{O}$), the name of the authors, and citation of the paper.

Acknowledgement

The authors thank Prof. A. Möller, Institute of Inorganic Chemistry, University of Cologne, for measurement of absorption spectra.

References

- [1] C. A. Ebberts, L. D. DeLoach, M. Webb, D. Eimerl, S. P. Velsko, D. A. Keszler, *IEEE J. Quantum Electron.* **1993**, *29*, 497–507.
- [2] H. Hellwig, S. Rühle, P. Held, L. Bohatý, *J. Appl. Crystallogr.* **2000**, *33*, 380–386.
- [3] A. G. Vigdorichik, Y. A. Malinovskii, A. G. Dryuchko, V. B. Kalinin, I. A. Verin, S. Y. Stefanovich, *Sov. Phys. Crystallogr.* **1992**, *37*, 783–791.
- [4] N. Audebrand, J. P. Auffrédic, M. Louër, N. Guillou, D. Louër, *Solid State Ionics* **1996**, *84*, 323–333.
- [5] M. G. Wyrouboff, *Bull. Soc. Franc. Minéral.* **1907**, *30*, 299–323.
- [6] M. C. Marignac, *Ann. Chim. Phys. (Sér. 4)* **1873**, *30*, 45–69.
- [7] M. H. Dufet, *Bull. Soc. Franc. Minéral.* **1888**, *11*, 143–148.
- [8] E. H. Kraus, *Z. Kristallogr.* **1901**, *34*, 397–431.
- [9] A. Fock, *Z. Kristallogr.* **1894**, *22*, 29–42.
- [10] P. Groth, *Chemische Kristallographie*, Wilhelm Engelmann, Leipzig, **1908**, vol. 2, pp. 152–155.
- [11] B. Eriksson, L. O. Larsson, L. Niinistö, *Acta Chem. Scand. A* **1982**, *36*, 465–470.
- [12] G. Meyer, E. Manek, A. Reller, *Z. Anorg. Allg. Chem.* **1990**, *591*, 77–86.
- [13] M. Najafpour, P. Starynowicz, *Acta Crystallogr., Sect. E* **2006**, *62*, i145–i146.
- [14] G. Jantsch, S. Wigdorow, *Z. Anorg. Chem.* **1911**, *69*, 221–231.
- [15] A. G. Vigdorichik, Y. A. Malinovskii, A. G. Dryuchko, *Sov. Phys. Crystallogr.* **1990**, *35*, 823–825.
- [16] P. Held, H. Hellwig, S. Rühle, L. Bohatý, *J. Appl. Crystallogr.* **2000**, *33*, 372–379.
- [17] M. V. Hobden, *J. Appl. Phys.* **1967**, *38*, 4365–4372.
- [18] Z. K. Odinets, N. A. Sal'nikova, A. K. Molotkin, T. N. Ivanova, *Russ. J. Inorg. Chem.* **1989**, *34*, 467–470.
- [19] B. Edlén, *Metrologia* **1966**, *2*, 71–80.
- [20] Enraf–Nonius, *MACH3 EXPRESS* **1989**, Delft, The Netherlands.
- [21] L. J. Farrugia, *J. Appl. Crystallogr.* **1999**, *32*, 837–838.
- [22] G. M. Sheldrick, *Acta Crystallogr., Sect. A* **2008**, *64*, 112–122.

Received: December 18, 2008
Published Online: June 10, 2009